The Journal of Neuroscience, December 15, 1997, 17(24):9554–9564

Measurement of Intracellular Free Zinc in Living Cortical Neurons: Routes of Entry

Stefano L. Sensi, Lorella M. T. Canzoniero, Shan Ping Yu, Howard S. Ying, Jae-Young Koh, Geoffrey A. Kerchner, and Dennis W. Choi

Center for the Study of Nervous System Injury and Department of Neurology, Washington University School of Medicine, St. Louis, Missouri 63110

We used the ratioable fluorescent dye mag-fura-5 to measure intracellular free Zn^{2+} ($[Zn^{2+}]_i$) in cultured neocortical neurons exposed to neurotoxic concentrations of Zn^{2+} in concert with depolarization or glutamate receptor activation and identified four routes of Zn^{2+} entry. Neurons exposed to extracellular Zn^{2+} plus high K^+ responded with a peak cell body signal corresponding to a $[Zn^{2+}]_i$ of 35–45 nM. This increase in $[Zn^{2+}]_i$ was attenuated by concurrent addition of Gd^{3+}, verapamil, ω-conotoxin GVIA, or nimodipine, consistent with Zn^{2+} entry through voltage-gated Ca^{2+} channels. Furthermore, under conditions favoring reverse operation of the Na^+–Ca^{2+} exchanger, Zn^{2+} application induced a slow increase in $[Zn^{2+}]_i$ and outward whole-cell current sensitive to benzamil–amiloride. Thus, a second route of Zn^{2+} entry into neurons may be via transporter-mediated exchange with intracellular Na^+. Both NMDA and kainate also induced rapid increases in neuronal $[Zn^{2+}]_i$. The NMDA-induced increase was only partly sensitive to Gd^{3+} or to removal of extracellular Na^+, consistent with a third route of entry directly through NMDA receptor-gated channels. The kainate-induced increase was highly sensitive to Gd^{3+} or Na^+ removal in most neurons but insensitive in a minority subpopulation ("cobalt-positive cells"), suggesting that a fourth route of neuronal Zn^{2+} entry is through the Ca^{2+}-permeable channels gated by certain subtypes of AMPA or kainate receptors.

Key words: mag-fura-5; voltage-gated calcium channels; sodium–calcium exchanger; calcium; sodium; glutamate; AMPA; NMDA; neurotoxicity; global ischemia; hypoxia

Zinc is required by all cells, playing a critical role in the control of gene transcription and metalloenzyme function (Vallee and Falchuk, 1993; Berg and Shi, 1996). In addition, Zn^{2+} likely serves as a mediator of cell–cell signaling in the CNS (Frederickson, 1989; Frederickson and Moncrieff, 1994). The mammalian brain contains a high concentration of histochemically reactive Zn^{2+}, primarily localized to glutamatergic terminals (Danscher, 1984; Perez-Clausell and Danscher, 1985) and released with neuronal activity (Howell et al., 1984). Endogenously released Zn^{2+} may reach 100 μM concentrations in the extracellular space (Assaf and Chung, 1984) and alter the behavior of multiple channels and receptors (Harrison and Gibbons 1994; Smart et al., 1994), in particular inhibiting NMDA receptors (Peters et al., 1987; Westbrook and Mayer, 1987; Christine and Choi, 1990).

Furthermore, intense exposure to Zn^{2+} can be neurotoxic, killing cortical neurons after several minutes (Yokoyama et al., 1986). This neurotoxicity appears also to be mediated by Zn^{2+} influx, in large part through voltage-gated Ca^{2+} channels and also through NMDA receptor-gated channels (Koh and Choi, 1994) and Ca^{2+}-permeable AMPA/kainate receptor-gated channels (Yin and Weiss, 1995). Pathophysiological relevance has been suggested by observations that brain Zn^{2+} translocates from presynaptic terminals into the postsynaptic cell bodies of neurons dying after prolonged seizures (Sloviter, 1985; Fredrickson et al., 1989) or transient global ischemia (Tonder et al., 1990; Koh et al., 1996), together with the finding that intraventricular administration of Ca-EDTA can attenuate global ischemia-induced neuronal death (Koh et al., 1996).

Although it would be useful to understand how neurons regulate intracellular cytosolic free Zn^{2+} concentrations ($[Zn^{2+}]_i$), at present, the tools available for measuring dynamic changes in $[Zn^{2+}]_i$ are limited. The Zn^{2+}-selective fluorescent dye 6-methoxy-8-*p*-toluene sulfonamide quinoline (TSQ) has provided valuable qualitative information about the location of chelatable Zn^{2+} in cells and tissues (Frederickson et al., 1987; Weiss et al., 1993), but limitations of solubility as well as possible complex interactions with membrane-bound Zn^{2+} have precluded quantitative measurement of $[Zn^{2+}]_i$ (Andrews et al., 1995). Recently, other sulfonamide derivatives of quinoline have been developed: (1) TFLZn, which has been used to detect $[Zn^{2+}]$ in synaptic terminals in hippocampal slices (Budde et al., 1997), in which high levels of Zn^{2+} are present (Frederickson, 1989); and (2) zinquin, which has been used to detect $[Zn^{2+}]_i$ in thymocytes, pancreatic islet cells, and hepatocytes (Zalewski et al., 1993, 1994; Brand and Kleineke, 1996). However, significant limitations are posed by the low affinity of these indicators for Zn^{2+} and, at least in the case of zinquin, by uneven intracellular distribution, perhaps reflecting sequestration. Other recently identified candidate Zn^{2+} indicators, Newport green and APTRA-BTC (Haugland, 1996), have promising specificity but low affinity.

Another approach to measuring $[Zn^{2+}]_i$ is to use fura-2-based, Ca^{2+}-sensitive ratioable fluorescent dyes. Fura-2 binds transition metals such as Zn^{2+} with much higher affinity than Ca^{2+}, producing a similar shift in emitted fluorescence (Grynkiewicz et al.,

Received May 15, 1997; revised Sept. 26, 1997; accepted Sept. 30, 1997.

This work was supported by National Institutes of Health Grant NS 30337 (D.W.C.). G.A.K. is an H. Hughes Medical Student Research Training Fellow. We thank D. Turetsky for assistance with the 293 cell line and Dr. K. Hyrc, Dr. M. Grabb, Dr. D. Lobner, and Dr. L. L. Dugan for helpful discussions.

S.L.S. and L.M.T C. contributed equally to this report.

Correspondence should be addressed to Dr. Dennis W. Choi, Department of Neurology, Box 8111, 660 South Euclid, St. Louis, MO 63110.

1985; Simons, 1993). Fura-2 itself has been used to monitor $[Zn^{2+}]_i$ in chromaffin cells (Vega et al., 1994), in myocytes and transfected cell lines (Atar et al., 1995), in bovine liver cells (Hechtenberg and Beyersmann, 1993), and in synaptosomes (Denny and Atchison, 1994), although confounding interference from changes in $[Ca^{2+}]_i$ is difficult to exclude.

In the present study, we explored the use of the related dye mag-fura-5 for real-time measurements of $[Zn^{2+}]_i$ in living cortical neurons. Simons (1993) reported that a similar analog, mag-fura-2, could be used to measure Zn^{2+} in solution over the 1–100 nM range, even in the presence of moderate Ca^{2+}, reflecting the higher affinity of the dye for Zn^{2+} (K_d = 20 nM) over Ca^{2+} or Mg^{2+}. We selected mag-fura-5 over mag-fura-2 because the former has additionally reduced affinity for Ca^{2+} or Mg^{2+} compared with mag-fura-2 (Haugland, 1996).

MATERIALS AND METHODS

Cell culture. Mixed cultures were prepared as described previously (Rose et al., 1993). Briefly, dissociated neocortices from embryo mice at 15–16 d gestation were plated in glass bottom 35 mm dishes (MatTek, Ashland, MA) at a density of three hemispheres/10 ml of plating medium containing 5% fetal bovine serum and 5% horse serum. Cultures were fed once a week with growth medium (5% horse serum). Videomicroscopy experiments were performed at 12–17 d *in vitro*.

$[Zn^{2+}]_i$ measurement. To monitor $[Zn^{2+}]_i$, cells were loaded with mag-fura-5 by incubation with mag-fura-5 AM at the concentration of 3 μM for 10 min in a HEPES-buffered solution containing (in mM): NaCl 120, KCl 5.4, $MgCl_2$ 0.8, HEPES 20, glucose 15, $CaCl_2$ 1.8, and NaOH 10, pH 7.4, at room temperature. Cells were washed and incubated for an additional 20 min in the HEPES-buffered solution. After loading, neurons were washed twice with the same solution, but lacking Mg^{2+} and Ca^{2+}. Na^+-free solutions were made by substituting NaCl and NaOH with equimolar amounts of *N*-methyl-D-glucamine (NMDG) and adjusting the pH to 7.4 with HCl.

All experiments were performed at room temperature under constant perfusion (2 ml/min) on the stage of a Nikon Diaphot inverted microscope equipped with a 75 W Xenon lamp and a Nikon 40×, 1.3 numerical aperture, epifluorescence oil immersion objective. Light was passed through 340 and 380 nm excitation filters mounted on a filter wheel with a computer-controlled filter driver. To avoid photobleaching of the cells under observation, the fluorescence intensity was attenuated with neutral density filters. The light was then reflected off a dichroic mirror (450 nm) and passed through a 510 nm emission filter.

Images were acquired with an intensified CCD camera (Quantex) and digitized using a Metafluor 2.5 software (Universal Imaging, West Chester, PA). Background fluorescence was subtracted from both (340 and 380 nm) images at the beginning of each experiment.

To determine the K_d of mag-fura-5 for Zn^{2+}, we recorded excitation spectra of mag-fura-5 free acid (1 μM) solution containing (in mM): KCl 100, EGTA 0.1, and 4-morphoinepropanesulfonic acid 10, pH 7, in a spectrofluorimeter (LS 50; Perkin-Elmer, Norwalk, CT) at room temperature. Various $ZnCl_2$ concentrations (from 0 to 0.2 mM) were added to the calibrating solution via a micrometer syringe (Hamilton, Reno, NV).

To calculate free Zn^{2+} concentration, we used Microsoft Excel (Solver) and the following equation: $[Zn^{2+}] = K_d$ [ZnEGTA]/[EGTA], where a dissociation constant (K_d) of EGTA for Zn^{2+} of 7.09 nM at pH 7 was taken and modified by 0.02 log unit per 0.01 increase in pH (Grynkiewiecz et al., 1985). K_d of mag-fura-5 for Zn^{2+} was obtained by plotting the log $[(F - F_{min})/(F_{max} - F)]$ versus the log of free $[Zn^{2+}]$ (Grynkiewicz et al., 1985), where F, F_{min}, and F_{max} are the fluorescence intensity values obtained with an excitation of 380 nm at each $[Zn^{2+}]$, at $[Zn^{2+}] = 0$, and at saturating $[Zn^{2+}]$, respectively. This plot gives an x-intercept of 7.56, so K_d = 27 nM (Fig. 1).

This K_d value of 27 nM was used in the ratio formula: $[Zn^{2+}] = K_d \cdot S_{f2}/S_{b2} \cdot [(R - R_{min})/(R_{max} - R)]$, where R is the observed 340/380 fluorescence ratio (Grynkiewicz et al., 1985), R_{min} is the 340/380 fluorescence ratio value determined in mag-fura-5-loaded cortical neurons exposed to 0 Zn^{2+} and 100 μM *N*,*N*′,*N*′-tetrakis (2-pyridylmethyl) ethylenediamine (TPEN), and R_{max} is 340/380 fluorescence ratio value determined in mag-fura-5-loaded cortical neurons exposed to 20 μM of the selective Zn^{2+} ionophore Na^+-pyrithione in the presence of 1 mM Zn^{2+}. S_{f2} indicates the fluorescence intensity at 380 at R_{min}; S_{b2} indicates the fluorescence intensity at 380 at R_{max}.

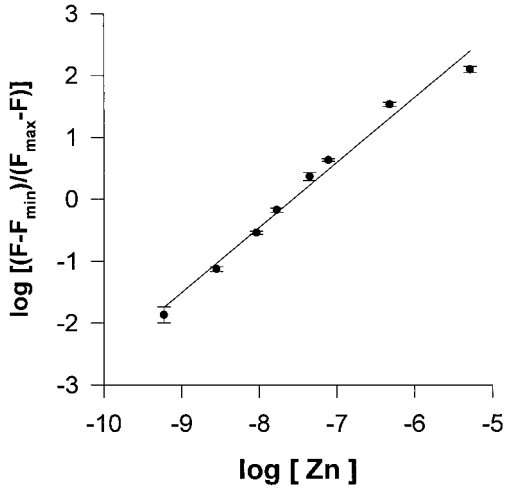

Figure 1. K_d of mag-fura-5 for Zn^{2+}. Hill plot analysis derived from plotting the log $[(F - F_{min})/(F_{max} - F)]$ versus the log of free $[Zn^{2+}]$. Values were obtained by using a mag-fura-5-free acid solution at various $[Zn^{2+}]$, as described in Materials and Methods. Each *point* represents the mean ± SEM from four different experiments.

Zinquin-ethyl ester (excitation, 380 nm; emission, 510 nm), APTRA-BTC (excitation, 380/440; emission, 510 nm), and Newport green diacetate (excitation, 495 nm; emission, 530 nm) were tested by using the same microscope setting equipped with the appropriate set of filters.

Whole-cell recording of Na^+–Ca^{2+} exchanger current. A 35 mm culture dish was used as a recording chamber on the stage of an inverted microscope (Nikon). Neurons of 15–20 μm diameter, with phase-bright cell bodies, were chosen for recordings. Neuronal identity has been confirmed previously by Nissl staining and electrophysiological characterization (Choi et al., 1987). Patch electrodes had a tip resistance of 10–15 MΩ (fire-polished). Voltage clamp was achieved by using an EPC-7 amplifier (List Electronic, Darmstadt, Germany). Series resistance compensation and capacitance compensation were routinely applied. Whole-cell current was sampled digitally at 500 μsec. The current signals were filtered by a 3 kHz, three-pole Bessel filter. Current traces were displayed and stored on a Macintosh computer (Quatra 950; Apple, Santa Clara Valley, CA) using the data acquisition and analysis program PULSE (HEKA Electronik, Pfalz, Germany). To test Zn^{2+}-activated membrane current, solutions were delivered to the selected neuron body via pressure ejection from a delivery pipette of 100 μm internal diameter placed ~100 μm from the cell body, using the DAD-12 superfusion system (Adams & List, Westbury, NY). The extracellular solution contained (in mM): NMDG 120, HEPES 10, and D-glucose 10, with or without $ZnCl_2$ 1. The pipette solution contained (in mM): NaCl 60, Cs-acetate 70, $CaCl_2$ 4.2, Mg_2-ATP 2, BAPTA 10, and HEPES 10. In addition, TTX (0.5 μM), TEA (5 mM), nifedipine (10 μM), and ouabain (20 μM) were included regularly in extracellular solutions to block Na^+ channels, K^+ channels, dihydropyridine-sensitive Ca^{2+} channels, and Na^+/K^+ ATPase, respectively. Solution pH was adjusted to 7.3 by adding HCl or NaOH as needed. Neuronal input resistance was measured at −70 and −10 mV, using an external solution containing (in mM): NaCl 124, KCl 5, TTX 0.002, HEPES 20, and glucose 15, with or without $MgCl_2$ 0.8 and $CaCl_2$ 2; and an internal solution containing (in mM): KCl 140, $MgCl_2$ 2, HEPES 10, and BAPTA 0.3.

Cobalt staining. After Zn^{2+}-imaging experiments, Co^{2+} uptake was performed as described previously (Turetsky et al., 1994). Cells were exposed to 100 μM kainate plus 5 mM $CoCl_2$ in uptake buffer containing (in mM): sucrose 139, NaCl 57.5, KCl 5, $MgCl_2$ 2, $CaCl_2$ 1, glucose 12, and HEPES 10, pH 7.6, for 30 min at room temperature. Cultures were then washed with uptake buffer plus 3 mM EDTA to remove extracellular Co^{2+} and incubated in 0.12% $(NH_4)_2S$ for 5 min to precipitate intracellular Co^{2+}. After three washes in uptake buffer, cells were fixed in 4% paraformaldehyde for 30 min. For silver enhancement, cultures were washed three times in development buffer (in mM: sucrose 292, hydroquinone 15.5, and citric acid 42) and incubated in 0.1% $AgNO_3$ in

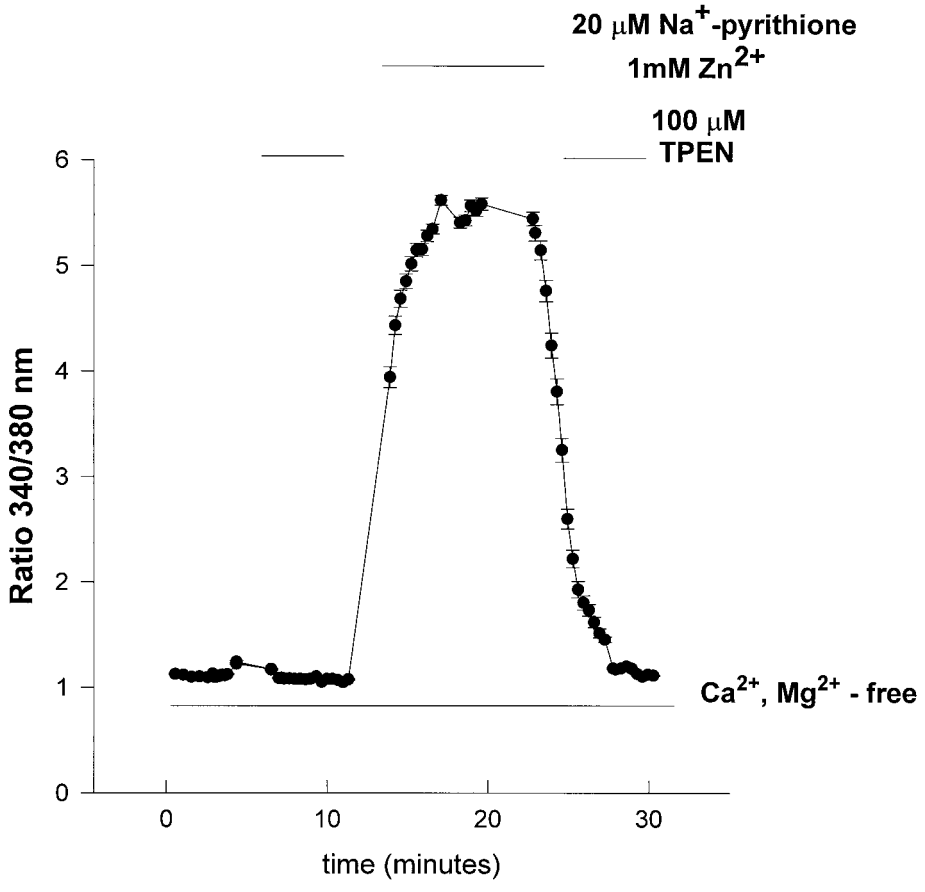

Figure 2. Calibration of mag-fura-5 detection of $[Zn^{2+}]_i$ in cortical neurons. Cortical neurons were loaded with mag-fura-5 and bathed in medium lacking Ca^{2+} or Mg^{2+}. At the indicated times, 20 μM Na^+-pyrithione plus 1 mM Zn^{2+} or 100 μM TPEN were added by bath perfusion, and the 340/380 nm fluorescence ratio was determined (mean ± SEM, $n = 24$ cells). Experiment is representative of three.

development buffer at 50°C on a slide warmer. This solution was changed at 15 min intervals, and enhancement was monitored periodically by microscopic observation. When enhancement was complete (usually after 45–50 min), the reaction was terminated by washing three times in warm development buffer. Once stained, fields were relocated by an independent observer lacking knowledge of the fluorescence results.

Statistics. Comparisons were obtained by ANOVA followed by Student–Newman–Keuls' test ($p < 0.05$).

Materials. APTRA-BTC-AM, mag-fura-5 AM, fura-2, Newport green diacetate, and 4-bromo (br)-A23187 were obtained from Molecular Probes (Eugene, OR). Na^+-pyrithione, Ca-EDTA, $ZnCl_2$, and TPEN were obtained from Sigma (St. Louis, MO). Zinquin-ethyl ester was obtained from Dojindo (Kumamoto, Japan).

RESULTS

Measurements of intracellular free Zn^{2+} in cortical neurons

Before settling on mag-fura-5, we explored the possible use of zinquin, Newport green, APTRA-BTC, or fura-2 in measuring $[Zn^{2+}]_i$ in cultured cortical neurons.

After 1 hr loading at 37°C with 25 μM zinquin-ethyl ester, cortical cultures exposed to 300 μM kainate plus 300 μM Zn^{2+} did not show a detectable increase in neuronal somatic zinquin fluorescence. Even exposure to the Zn^{2+} ionophore 20 μM Na^+-pyrithione plus 1 mM Zn^{2+} did not yield a zinquin signal, suggesting that the dye was not adequately loaded or cleaved. As a control, zinquin-loaded HEK 293 cells exposed to the same ionophore plus Zn^{2+} did exhibit a large increase in fluorescence, albeit distributed unevenly within the cells (data not shown).

Two other Zn^{2+}-selective dyes, Newport green and APTRA-BTC, were loaded successfully into cortical neurons and exhibited strong responses to Zn^{2+} ionophore treatment. However, consistent with their low affinities for Zn^{2+} (see above), minimal responses were detectable after the physiological (probably pathophysiological) stimulus, 500 μM kainate plus 300 μM Zn^{2+}. We also examined the use of fura-2 to detect intracellular Zn^{2+}. However, beside the high sensitivity of fura-2 for Ca^{2+}, fura-2 also appeared too sensitive to Zn^{2+} for our purposes (K_d for Zn^{2+}, ~2 nM) (Grynkiewicz et al., 1985). We found that fura-2-loaded neurons exhibited a near saturating response to exposure to 300 μM kainate plus 300 μM Zn^{2+} (in the absence of extracellular Ca^{2+}).

As described above, we loaded mixed neuronal and glial cortical cell cultures with mag-fura-5 AM at a concentration of 3 μM for 10 min at room temperature. Dye concentrations between 1 and 10 μM were explored, 1 μM being too little for reliable measurements, and 10 μM yielding reduced responses compared with 3 or 5 μM, suggestive of buffering (data not shown). Because neuronal cell bodies sat well above the underlying glial layer, it was possible to detect the 340/380 fluorescence ratio originating in these cell bodies with minimal interference from underlying glia. At rest, the neuronal somatic 340/380 fluorescence ratio was ~1 and insensitive to application of the membrane-permeant selective Zn^{2+} chelator TPEN (100 μM) (Arslan et al., 1985) (Fig. 2, R_{min}). Application of the selective Zn^{2+} ionophore 20 μM Na^+-pyrithione (Zalewski et al., 1993), together with 1 mM Zn^{2+} in HEPES buffer lacking Ca^{2+} and Mg^{2+}, produced an increase in the neuronal somatic 340/380 fluorescence ratio to 5.6 (Fig. 2, R_{max}). If extracellular Zn^{2+} was omitted, no signal was seen (data not shown). Reapplication of 100 μM TPEN produced a rapid fall in the 340/380 fluorescence signal back to baseline (Fig. 2).

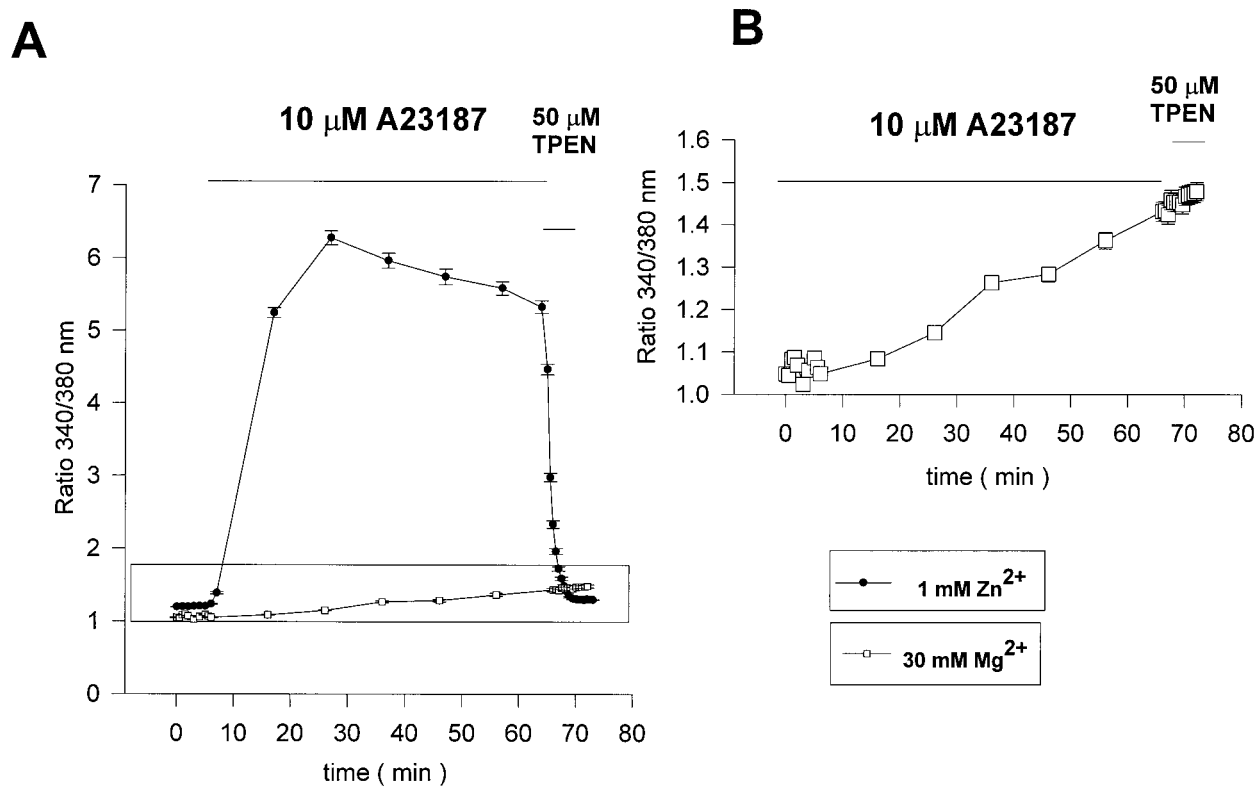

Figure 3. Comparison of mag-fura-5 sensitivity to Mg^{2+} and Zn^{2+}. *A*, Exposure to br-A23187 (10 μM) for 60 min in the presence of 30 mM Mg^{2+} (*open symbols*) or 1 mM Zn^{2+} (*solid symbols*). TPEN (50 μM) was added at the indicated time to quench the Zn^{2+} signal. *B*, Inset showing the same Mg^{2+} signal as in *A*, but at higher vertical gain; TPEN has no effect. Each *point* is the mean ± SEM of at least 30 cells. Experiment is representative of three.

We considered it unlikely that this somatic mag-fura-5 signal was confounded by Ca^{2+} detection, given the absence of extracellular Ca^{2+} and the low affinity of the dye for Ca^{2+} (see above). Indeed, previous studies with mag-fura-2 or mag-fura-5 did not detect neuronal somatic Ca^{2+} after glutamate exposure or electrical stimulation, even with extracellular Ca^{2+} present (Brocard et al., 1993; Petrozzino et al., 1995). A more serious possible confounding effect could derive from changes in intracellular Mg^{2+}, which are in the millimolar range and may be increased by glutamate receptor activation even in the absence of extracellular Mg^{2+} (Brocard et al., 1993). However, consistent with the studies of Illner et al. (1992), even exposure to 30 mM Mg^{2+} in the presence of an ionophore, br-A23187, produced only a small change in the neuronal somatic 340/380 fluorescence ratio compared with the large change produced by Zn^{2+} in the same cells (Fig. 3). As a control, we demonstrated that the large Zn^{2+} signal, but not the small Mg^{2+} signal, was sensitive to application of 50 μM TPEN (Fig. 3).

Depolarization and Na^+-dependent pathways involved in $[Zn^{2+}]_i$ elevation

Next we used mag-fura-5 to measure in cortical neurons accumulating Zn^{2+} under depolarizing conditions that might have pathophysiological relevance. Mixed cortical cell cultures were loaded with mag-fura-5 as above and placed into HEPES buffer lacking Ca^{2+} and Mg^{2+} (no chelators were added). The removal of external Ca^{2+} and Mg^{2+} produced no significant change (<20% change in the mean. $p > 0.05$ with $n = 4$ cells per condition) in the input resistance of the neurons either in resting condition (−70 mV) or after depolarization (−10 mV). Application of 30–90 mM KCl plus 300 μM Zn^{2+} for 15 sec elicited a K^+ concentration-dependent and persistent (lasting >60 min) increase in $[Zn^{2+}]_i$ to 48 ± 1.02 nM that was terminated by application of 50 μM TPEN, whereas application of 90 mM KCl alone produced no response (Fig. 4*A*,*B*). The response to 90 mM KCl could be blocked completely by concurrent application of the nonselective voltage-gated Ca^{2+} channel blockers gadolinium (Gd^{3+}, 10 μM) and verapamil (100 μM) and partially blocked by the selective blockers ω-conotoxin GVIA (100 nM) and nimodipine (1 μM) (Fig. 4*C*). The observed reduction of the fluorescence produced by Gd^{3+} was not attributable to quenching, because the signal induced by exposure to Na^+-pyrithione was not affected by 10 μM Gd^{3+} (data not shown).

Inclusion of 1.8 mM Ca^{2+}, alone or together with 0.8 mM Mg^{2+}, in the bathing medium reduced by approximately half the peak $[Zn^{2+}]_i$ response (sensitive to TPEN) induced by application of 90 mM KCl plus 300 μM Zn^{2+} (Fig. 4*C*). To test the hypothesis that Zn^{2+} might also enter neurons via reverse operation of an exchanger similar (or identical) to the Na^+–Ca^{2+} exchanger, we loaded neurons with Na^+ by exposing the cultures to 1 mM ouabain for 15 min. Removal of extracellular Na^+ (replaced with 130 mM NMDG), together with application of 100 μM Zn^{2+}, still in the presence of ouabain, then produced over several minutes a slowly progressive increase in neuronal somatic $[Zn^{2+}]_i$ (Fig. 5*B*) that was larger than that produced by application of 100 μM Zn^{2+} alone on control neurons (Fig. 5*A*). This enhanced increase in $[Zn^{2+}]_i$ was inhibited by the Na^+–Ca^{2+} exchanger blockers benzamil-amiloride (BNZ) (Fig. 5*C*) and D-methyl-benzamil-amiloride (100 μM) (data not shown). To avoid

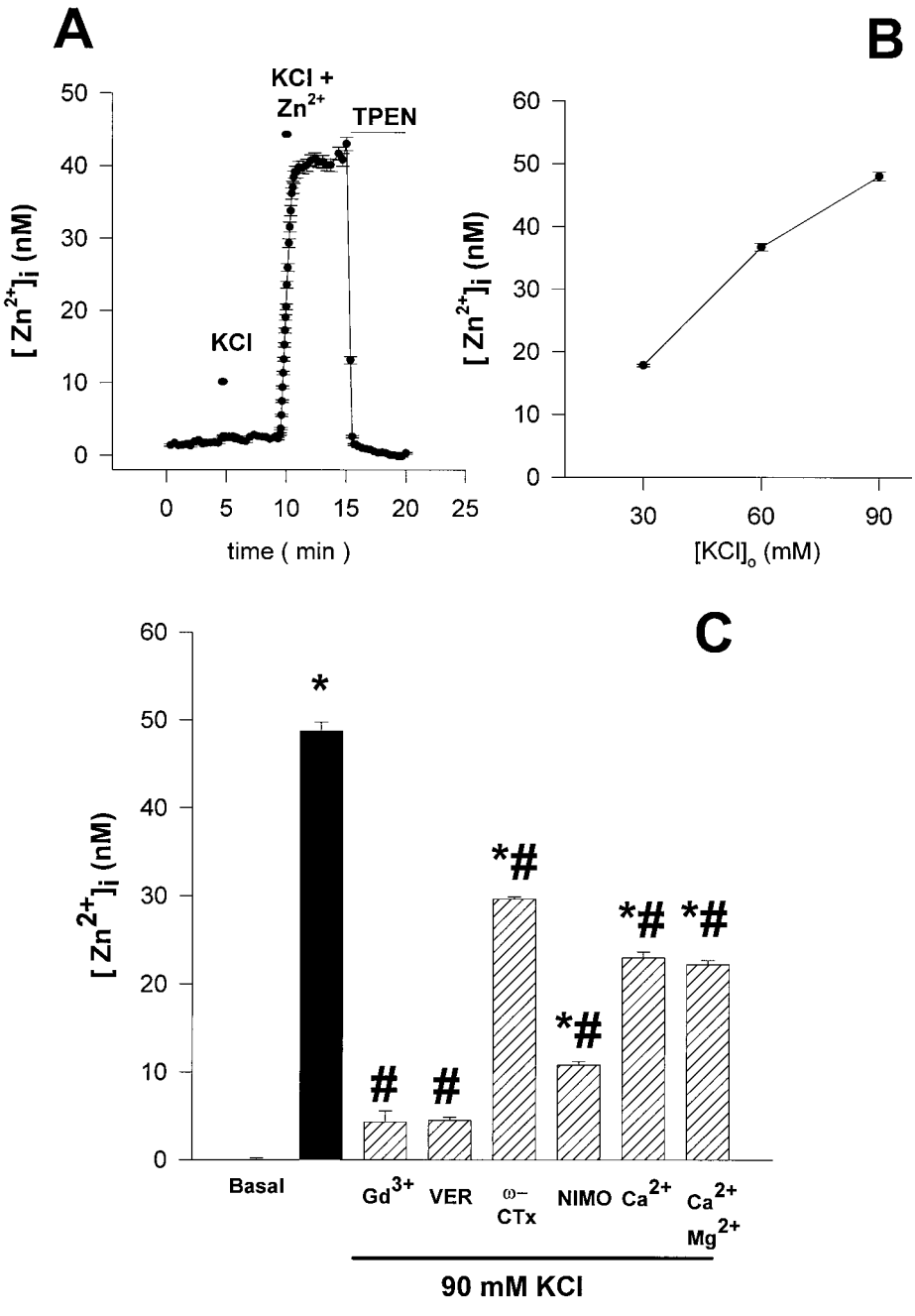

Figure 4. KCl evoked increase in $[Zn^{2+}]_i$. *A*, KCl (90 mM) was applied for 15 sec alone or in combination with 300 μM Zn^{2+}. TPEN (50 μM) was added 5 min after the exposure to Zn^{2+}. Each *point* is the mean ± SEM of 49 cells. Experiment is representative of nine. *B*, Concentration–response curve of KCl-induced $[Zn^{2+}]_i$. Neurons were exposed for 15 sec to indicated KCl concentrations. Each *point* is the mean ± SEM of the peak $[Zn^{2+}]_i$ levels obtained from at least three experiments. *C*, Pharmacological modulation of 90 mM KCl-induced increase in $[Zn^{2+}]_i$ in cortical neurons. $[Zn^{2+}]_i$ levels were measured before (*Basal*) or at the peak response after a 15 sec exposure to 90 mM KCl, alone or in the presence of 10 μM Gd^{3+}, 100 μM verapamil (*VER*), 100 nM ω-conotoxin-GVIA (ω-*CTx*), 1 μM nimodipine (*NIMO*), 1.8 mM Ca^{2+}, or 1.8 mM Ca^{2+} plus 0.8 mM Mg^{2+}. Each *column* is pooled from three to nine experiments involving at least 40 cells per experiment. *Asterisks* indicate difference from basal level; #, difference from KCl-stimulated level, as determined by ANOVA and Student–Newman–Keuls' test ($p < 0.05$).

activation of voltage-gated Ca^{2+} channels and glutamate receptors, 10 μM Gd^{3+}, 10 μM MK-801, and 10 μM NBQX were present throughout the experiment. No detectable increase in $[Zn^{2+}]_i$ was produced by brief (15 sec) application of an Na^+-free solution containing 100–300 μM Zn^{2+}.

To confirm that reversed operation of a neuronal exchanger like the Na^+–Ca^{2+} exchanger could mediate Zn^{2+} influx, we used whole-cell voltage clamp to record the membrane current associated with the electrogenic exchanger operation. Under conditions favoring reverse operation, but limited by lack of extracellular Ca^{2+} (0 Na^+, 0 Ca^{2+} in the bath; 60 mM Na^+, 0 Ca^{2+} in the pipette), local application of 1 mM extracellular Zn^{2+} produced a reversible outward current shift (23.0 ± 4.4 pA at −40 mV, SEM; $n = 4$ cells) (Fig. 6), resembling the Na^+–Ca^{2+} exchanger current induced by Ca^{2+} under the same conditions (Yu and Choi, 1997). This Zn^{2+}-induced membrane current was blocked 70% by 100 μM BNZ (7.7 ± 3.2 pA, SEM; $n = 4$ cells) (Fig. 6) and was totally blocked by 300 μM BNZ ($n = 7$ cells) (data not shown). Furthermore, the current was not observed if Na^+ was removed from the pipette solution (data not shown).

Modulation of $[Zn^{2+}]_i$ in response to glutamate agonists

Application of NMDA (10–300 μM, 15 sec) in the presence of 300 μM extracellular Zn^{2+} produced a quick increase in neuronal $[Zn^{2+}]_i$ in an NMDA concentration-dependent manner that was sensitive to the competitive NMDA antagonist D-APV (100 μM) (Fig. 7). A maximal $[Zn^{2+}]_i$ of 31 ± 0.97 nM was induced by 300 μM NMDA. This NMDA-induced increase in $[Zn^{2+}]_i$ was only

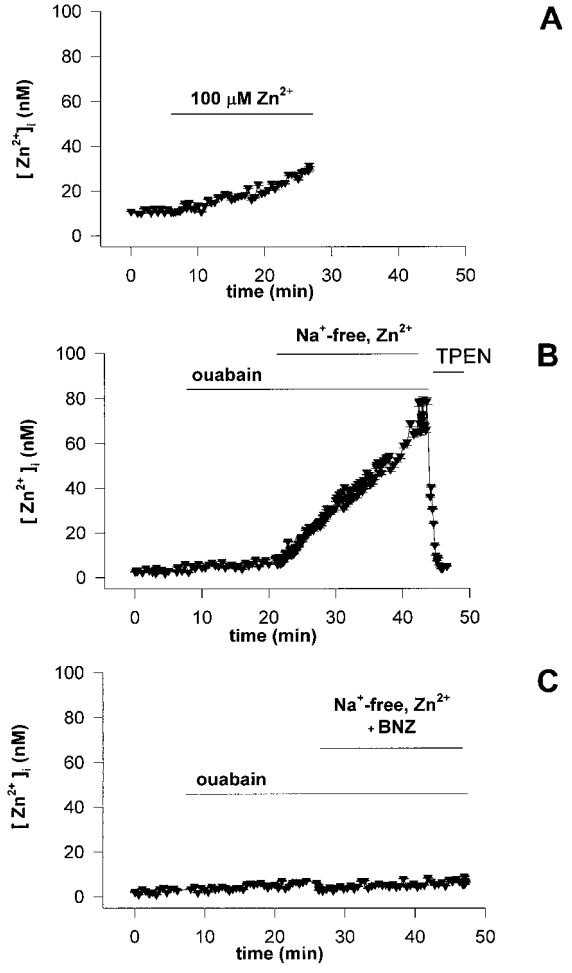

Figure 5. Na^+-dependent $\Delta[Zn^{2+}]_i$. *A*, Fifteen minute exposure to 100 μM Zn^{2+} in the presence of 10 μM Gd^{3+}, 10 μM MK-801, and 10 μM NBQX produced a gradual increase in $[Zn^{2+}]_i$. Each *point* is the mean ± SEM of 58 cells in a single experiment, representative of three. *B*, Removal of extracellular Na^+ (equimolar substitution with NMDG) after the addition of 1 mM ouabain increases $\Delta[Zn^{2+}]_i$ induced by exposure to 100 μM Zn^{2+}. Each *point* is the mean ± SEM of 57 cells in a single experiment, representative of six. *C*, Same as in *B*, but with the addition of 100 μM BNZ. Each *point* is the mean ± SEM of 56 cells in a single experiment, representative of four.

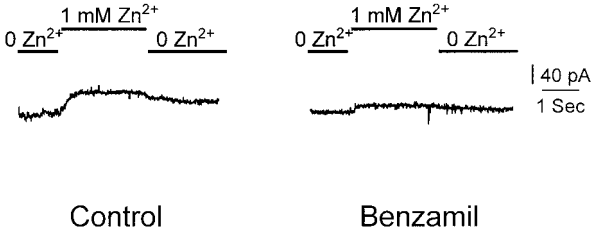

Figure 6. Exchanger current activated by external Zn^{2+} application. *Left*, Whole-cell recording from a cortical neuron in a bathing medium lacking Na^+ or Ca^{2+} (see Materials and Methods); the pipette solution contained 60 mM Na^+. $ZnCl_2$ (1 mM) was applied in the bath as indicated. Holding potential = −40 mV. Representative of four cells. *Right*, Same as in *left*, but with 100 μM BNZ in the bath. Representative of four cells.

partially sensitive to application of 10 μM Gd^{3+} or removal of extracellular Na^+ (NMDG replacement).

Application of kainate (10–300 μM, 15 sec) in the presence of

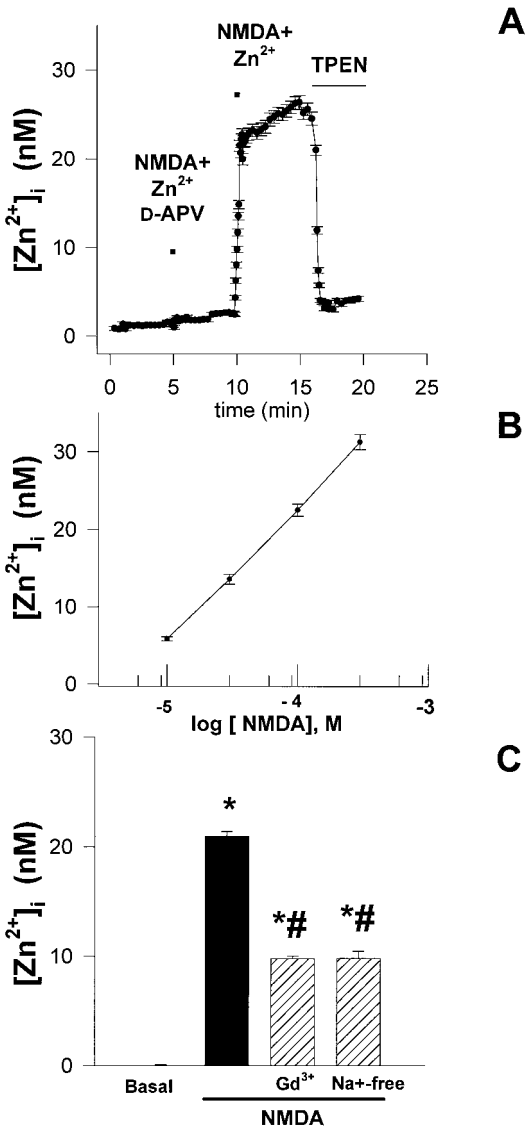

Figure 7. NMDA-induced increase in $[Zn^{2+}]_i$. *A*, NMDA (100 μM, 15 sec) was applied together with 300 μM Zn^{2+}, with or without 100 μM D-APV as indicated. TPEN (50 μM) was added as indicated. Each *point* is the mean ± SEM of 58 cells in a single experiment, representative of four. *B*, Concentration–response curve of NMDA-induced $\Delta[Zn^{2+}]_i$. The indicated concentrations of NMDA were applied for 15 sec in the presence of 300 μM Zn^{2+}, and the resultant peak increase in $[Zn^{2+}]_i$ was measured. Each *concentration point* was pooled from three experiments involving at least 40 cells per experiment; SEM bars are lost in the symbols. *C*, Pharmacological modulation of NMDA-induced $\Delta[Zn^{2+}]_i$. $[Zn^{2+}]_i$ levels were measured before (basal) or at the peak response after a 15 sec exposure to NMDA, in presence of 10 μM Gd^{3+} or in absence of extracellular Na^+ (NMDG). Each *column* is pooled from three to nine experiments involving at least 40 cells per experiment. *Asterisks* indicate difference from basal level; #, difference from NMDA-stimulated levels, as determined by ANOVA and Student–Newman–Keuls' test ($p < 0.05$).

300 μM extracellular Zn^{2+} also produced a quick increase in neuronal $[Zn^{2+}]_i$ in a concentration-dependent manner, sensitive to 10 μM NBQX (Fig. 8). To determine the extent to which the Zn^{2+} entry triggered by kainate receptor stimulation was mediated indirectly via voltage-gated Ca^{2+} channels, we exposed neurons to kainate in an Na^+-free solution (NMDG) (to prevent Na^+ entry-mediated membrane depolarization and consequent activation of voltage-gated Ca^{2+} channels).

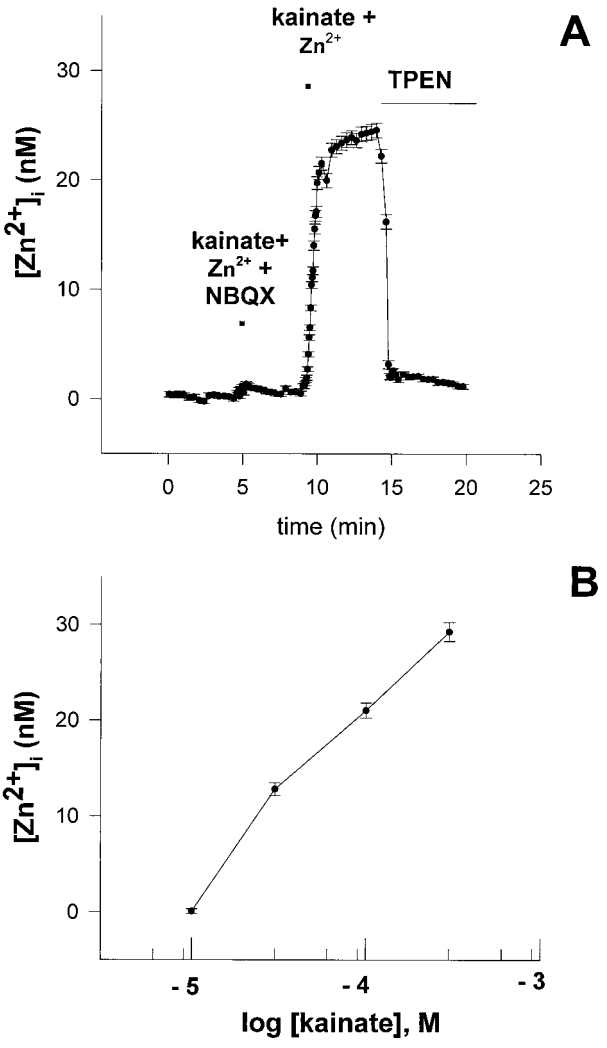

Figure 8. Kainate-induced $\Delta[Zn^{2+}]_i$. *A*, Kainate (100 μM, 15 sec) was applied together with 300 μM Zn^{2+}, with or without 10 μM NBQX as indicated. TPEN (50 μM) was added as indicated. Each *point* is the mean ± SEM of 61 cells in a single experiment representative of three. *B*, Concentration–response curve of kainate-induced elevation in $[Zn^{2+}]_i$. The indicated concentrations of kainate were applied for 15 sec in the presence of 300 μM of Zn^{2+}, and the resultant peak increase in $[Zn^{2+}]_i$ was measured. Each *concentration point* was pooled from three experiments involving at least 40 cells per experiment; SEM bars are lost in the symbols.

Removal of Na^+ inhibited kainate-induced increase in $[Zn^{2+}]_i$ in most, but not all, neurons. In three pooled experiments, application of 50 μM kainate in the Na^+-free solution caused $[Zn^{2+}]_i$ to rise strongly in 17 of 156 (10.8%) neurons (Fig. 9*A*,*B*). The microscope fields were marked, and the cultures were subsequently subjected to staining for kainate-activated cobalt uptake ("Co^{2+}-positive neurons"), a marker for the functional expression of AMPA or kainate receptors gating channels with high Ca^{2+} permeability (Pruss et al., 1991, Turetsky et al., 1994; Yin et al., 1994). There was a one-to-one correlation between strong $[Zn^{2+}]_i$-responsiveness in Na^+-free conditions and Co^{2+} positivity (Fig. 9, *C*,*D*).

Like the removal of extracellular Na^+, inhibition of voltage-gated Ca^{2+} channels with 10 μM Gd^{3+} or 1 μM nimodipine strongly attenuated the kainate-induced increase in $[Zn^{2+}]_i$ in most of the cells (Fig. 10). However, in a small number of neurons, the increase in $[Zn^{2+}]_i$ remained near the control value (Fig. 10), supporting the idea that Zn^{2+} influx also occurred directly through AMPA/kainate receptor-gated channels, possessing high Ca^{2+} permeability.

DISCUSSION

Taking a lead from Simons (1993), who used mag-fura-2 to measure Zn^{2+} concentrations in solution, we demonstrate here that mag-fura-5 can be used to follow $[Zn^{2+}]_i$ in living cortical neurons. Three lines of evidence indicate that the mag-fura-5 ratio signal we observed indeed reflects increases in $[Zn^{2+}]_i$. First, the signal was induced by application of a Zn^{2+}-selective ionophore, Na^+-pyrithione, only when extracellular Zn^{2+} was present. Second, this Na^+-pyrithione/Zn^{2+} signal was quenched rapidly by the specific cell-permeable Zn^{2+} chelator TPEN. Third, conclusions regarding routes of Zn^{2+} entry reached here are consistent with previous observations using TSQ fluorescence or $^{65}Zn^{2+}$ accumulation to assess Zn^{2+} influx.

The idea that depolarizing stimuli can drive Zn^{2+} entry through Gd^{3+}- and nimodipine-sensitive voltage-gated channels fits with toxicity experiments (Weiss et al., 1993; Freund and Reddig, 1994; Manev et al., 1997), as well as with recent experiments from our laboratory tracking depolarization-induced neuronal $^{65}Zn^{2+}$ influx in the same cultures (H. S. Ying, S. Farhangrazi, C. S. Ling, D. Lobner, L. M. T. Canzoniero, S. L. Sensi, J. Y. Koh, C. T. Sheline, and D. W. Choi, unpublished observations). Although Zn^{2+}, like other transition metals, is commonly considered an inhibitor of Na^+ and Ca^{2+}-voltage-gated channels (Harrison and Gibbons, 1994), such inhibition does not exclude slow permeation. Zn^{2+} sheds its water of hydration at a speed intermediate between that of Ca^{2+} and Mg^{2+} (Diebler et al., 1969) and permeates through Ca^{2+} channels on invertebrate neurons (Fukuda and Kawa, 1977), chromaffin cells (Vega et al., 1994), and myocytes (Atar et al., 1995). Wang and Quastel (1990) attributed the complex effects of extracellular Zn^{2+} on acetylcholine release at the neuromuscular junction to permeation through nerve terminal Ca^{2+} channels. It will be interesting in the future to see whether any subset of the voltage-gated channels passing Zn^{2+} prefer Zn^{2+} over Ca^{2+} and are really thus "Zn^{2+} channels."

The idea that Zn^{2+} can also permeate through NMDA receptor-gated Ca^{2+} channels (Koh and Choi, 1994) is supported by present data showing that the NMDA-induced $[Zn^{2+}]_i$ signal was only partly sensitive to Gd^{3+} addition or extracellular Na^+ removal. The speed of this response (seconds) argues against any large mediation by exchange with Na^+, a mechanism requiring several minutes to produce substantial elevations in $[Zn^{2+}]_i$ (see below). Zn^{2+} mediates a voltage-sensitive, fast flicker block of NMDA receptor-gated channels (Christine and Choi, 1990). Possibly, the onset of this block reflects plugging of the channel by Zn^{2+}, and relief of block reflects permeation of Zn^{2+}.

It is likely that Zn^{2+} similarly passes through the Ca^{2+}-permeable AMPA/kainate receptors expressed on a small minority of cortical neurons, the "cobalt-positive" cells (Pruss et al., 1991; Turetsky et al., 1994), reflecting (in the case of AMPA receptors) lack of an edited form of GluRB/GluR2 (Hollmann et al., 1991; Verdoorn et al., 1991). This conclusion fits with that reached by Yin and Weiss (1995), who used TSQ to assess $[Zn^{2+}]_i$ qualitatively. Recent evidence suggests that cobalt-positive cortical neurons are primarily GABAergic interneurons (Jonas et al., 1994; Yin et al., 1994), raising the interesting

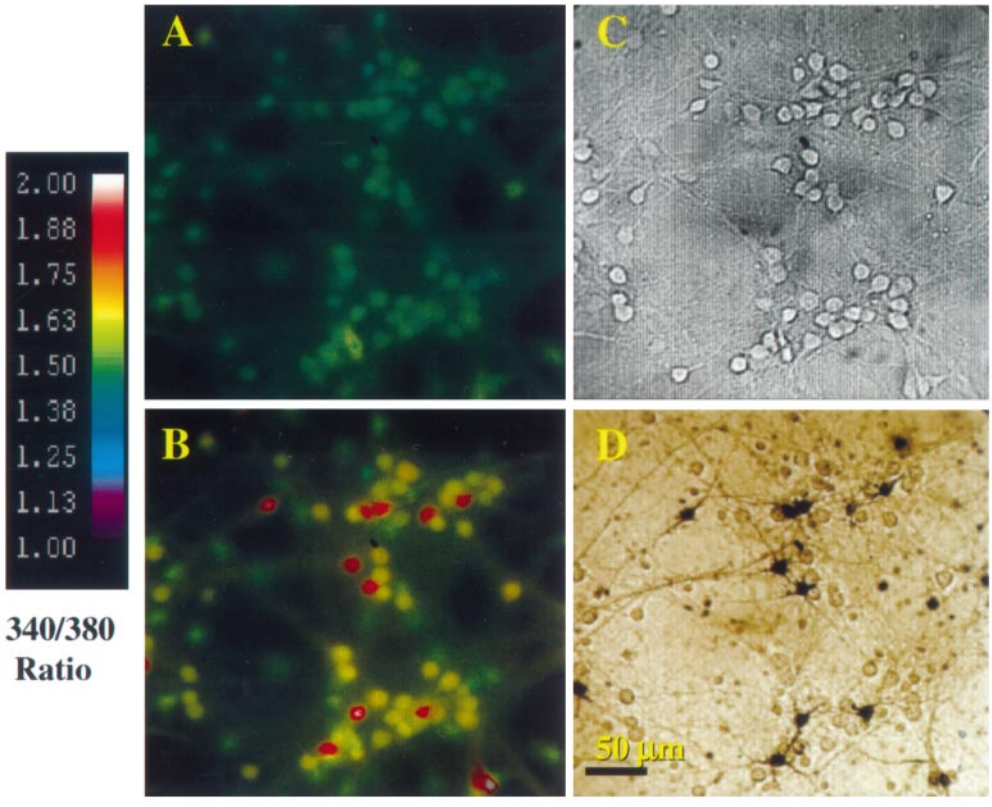

Figure 9. $[Zn^{2+}]_i$ elevation in cobalt-positive neurons. *A*, *B*, Pseudocolor images depicting $[Zn^{2+}]_i$, as mag-fura-5 340/380 ratio values as indicated in the *scale*, in cortical neurons before (*A*) and after (*B*) exposure (15 sec) to 50 μM kainate in the presence of 100 μM Zn^{2+} but in the absence of extracellular Na^+ (NMDG replacement). $[Zn^{2+}]_i$ elevation in a minority subpopulation of neurons can be seen. *C*, Phase-contrast micrograph of the same field. *D*, Kainate-activated cobalt staining of the same field. A one-to-one correlation is seen between neurons responding with a large $\Delta[Zn^{2+}]_i$ in the absence of extracellular Na^+ and cobalt-positivity. Scale bar, 50 μm.

possibility that inhibitory interneurons may be especially vulnerable to Zn^{2+}-induced death under conditions in which AMPA receptors are activated. Furthermore, the ability of certain AMPA receptors to mediate toxic Zn^{2+} entry may provide a link between previous observations implicating AMPA receptor overactivation (Pellegrini-Giampietro et al., 1992; Sheardown et al., 1993) and Zn^{2+} entry (Koh et al., 1996) in selective neuronal death after transient global ischemia.

Beside entry through voltage- and agonist-gated Ca^{2+} channels, we provide evidence here for the possibility that Zn^{2+} may also enter depolarized neurons via BNZ-sensitive exchange with intracellular Na^+. Although it is possible that a unique "Na^+–Zn^{2+}" exchanger mediates Zn^{2+} entry in exchange for Na^+ efflux (or vice versa under different conditions), it is conservative to postulate that Zn^{2+} can substitute for Ca^{2+} in the operation of the known neuronal Na^+–Ca^{2+} exchanger (Blaustein et al., 1991, 1996; Yu and Choi, 1997), as shown for Sr^{2+} and Ba^{2+} in cardiac sarcolemmal vesicles (Tibbits and Philipson, 1985) and for Mn^{2+} and Cd^{2+} in ferret red blood cells (Frame and Milanick, 1991). Such exchanger-mediated Zn^{2+} entry would be favored when the normal membrane Na^+ gradient is diminished and membrane potential is depolarized, as occurs during brain ischemia. The outward current detected here in association with Zn^{2+} entry is consistent with the electrogenic nature of the exchanger, with a typical stochiometry of one Ca^{2+} (or Zn^{2+} ion) exchanged for three Na^+ ions.

We think it is unlikely that the mag-fura-5 signal measured here was substantially confounded by detection of Ca^{2+} or Mg^{2+}. In the absence of extracellular Ca^{2+}, previous studies have not suggested that $[Ca^{2+}]_i$ in neuronal soma would rise to the high micromolar levels needed to activate mag-fura-5 (K_d, ~20 μM) (Petrozzino et al., 1995). Mg^{2+} is a greater possibility, because intracellular levels at rest are in the 0.5–1 mM range (Brocard et al., 1993), already approaching the K_d of the dye for Mg^{2+} (2.6 mM) (Haugland, 1996). However, although some baseline Mg^{2+} binding is therefore probable, when we forced Mg^{2+} entry by increasing extracellular Mg^{2+} to 30 mM in the presence of a suitable ionophore, br-A23187, only small ratio shifts in mag-fura-5 fluorescence occurred, and these shifts, unlike the shifts induced by depolarizing neurons in the presence of extracellular Zn^{2+}, were insensitive to TPEN. We cannot absolutely rule out the complex possibility that Zn^{2+} entry somehow caused massive intracellular Mg^{2+} release analogous to the Ca^{2+}-triggered intracellular Mg^{2+} release delineated by Brocard et al. (1993). However, no elevation of $[Mg^{2+}]_i$ was seen by Brocard et al. (1993) in cortical neurons exposed to depolarizing conditions such as veratridine or kainate.

The nominal absence of Ca^{2+} or Mg^{2+} used in many of the present experiments to minimize confounding detection of Ca^{2+} or Mg^{2+} likely exaggerated Zn^{2+} influx by over that which would normally occur in the presence of physiological concentrations of these ions. The absence of extracellular Ca^{2+} can reduce the selectivity of calcium channels on frog muscle cells (Almers et al., 1984) or potassium channels on squid neurons (Armstrong and Barneo, 1987), although because we performed our experiments without added chelators, enough Ca^{2+} and Mg^{2+} may have been present to maintain channel selectivity. In any case, previous studies demonstrated that $[Ca^{2+}]_o$ inversely affects Zn^{2+} toxicity (Koh and Choi, 1994). Moreover, a direct inhibition of $^{65}Zn^{2+}$ influx by extracellular Ca^{2+} (IC_{50} = 416 μM; Hill coefficient = 1.01) has been demonstrated in our culture system (H. S. Ying, S. Farhangrazi, C. S. Ling, D. Lobner, L. M. T. Canzoniero, S. L. Sensi, J. Y. Koh, C. T. Sheline, and D. W. Choi, unpublished observations), and we found here a substantial decrease (~50%) in peak $[Zn^{2+}]_i$ when depolarization by 90 mM KCl was evoked in the presence of a physiological concentration (1.8 mM) of

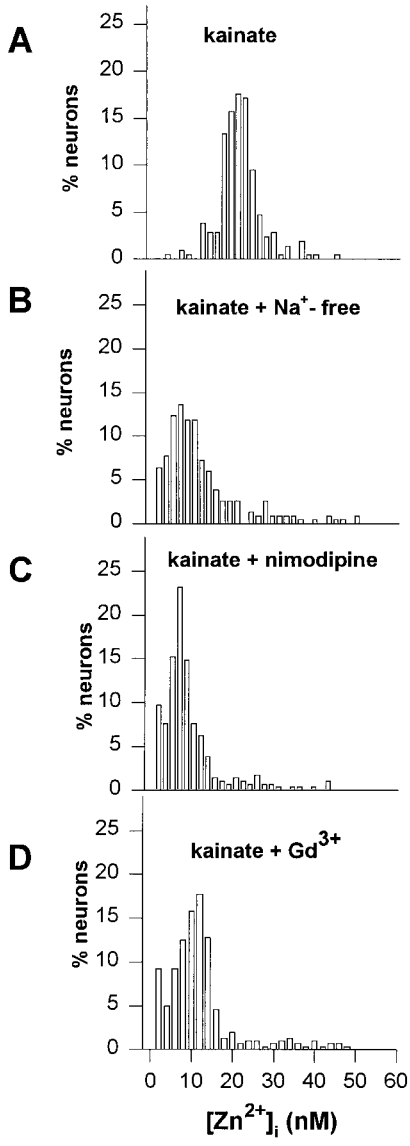

Figure 10. Pharmacological modulation of kainate-induced elevation in $[Zn^{2+}]_i$. *Histograms* show the fraction of the cortical neuronal population exhibiting the indicated peak $[Zn^{2+}]_i$ response during a 15 sec exposure to 100 μM kainate in the presence of 300 μM Zn^{2+}. *A*, Normal extracellular Na^+ (mean ± SEM, 23.5 ± 0.4 nM; $n = 210$ cells); *B*, in the absence of extracellular Na^+ (12.9 ± 0.8; $n = 235$); *C*, in the presence of 1 μM nimodipine (9.6 ± 0.5; $n = 289$ cells); *D*, in the presence of 10 μM Gd^{3+} (11.2 nM ± 0.5; $n = 305$ cells). For each condition, the data were pooled from at least three experiments. All the treated conditions were statistically different from the control condition, as determined by ANOVA and Student–Newman–Keuls' test ($p < 0.05$).

extracellular Ca^{2+} with or without 0.8 mM Mg^{2+}. However, present experiments may model conditions occurring in the ischemic brain *in vivo*, in which extracellular calcium dramatically drops (Hansen, 1985) and extracellular Zn^{2+} likely rises (Koh et al., 1996). That is, if we are correct in postulating that most of the mag-fura-5 fluorescence shift observed in the present experiments can be interpreted as an increase in $[Zn^{2+}]_i$, then present observations provide a direct estimate (10–30 nM) of neuronal somatic $[Zn^{2+}]_i$ under pathophysiological conditions of NMDA or kainate activation when extracellular Zn^{2+} is abundantly present and extracellular Ca^{2+} is low (Figs. 7, 8).

Such increases would be produced easily by the total Zn^{2+} accumulating in cultured cortical neurons exposed to high K^+ and 1 mM Zn^{2+}, as measured with atomic emission spectroscopy, which is sufficient to produce a calculated intracellular Zn^{2+} concentration of ~1 mM in the absence of Zn^{2+} sequestration or binding (H. S. Ying, S. Farhangrazi, C. S. Ling, D. Lobner, L. M. T. Canzoniero, S. L. Sensi, J. Y. Koh, C. T. Sheline, and D. W. Choi, unpublished observations). Most likely, the bulk of the Zn^{2+} entering depolarized neurons does not remain free in the cytosol, but rather is taken up into organelles (Palmiter et al., 1996) or binds to macromolecules such as metallothioneins (Masters et al., 1994; Ebadi et al., 1995; Maret, 1995). Erickson et al. (1997) demonstrated that deletion of the gene coding for metallothionein-III increased the CA3 neuronal death associated with kainate-induced seizures, a process likely mediated at least in part by toxic zinc translocation from mossy fiber terminals into CA3 neurons (Sloviter, 1985; Koh et al., 1996) (S. W. Suh, J. Y. Koh, and D. W. Choi, unpublished observations). Furthermore, present measurements of somatic fluorescence would not be expected to detect Zn^{2+} entering in neurites.

Previous determinations of $[Zn^{2+}]_i$ in nonneuronal cells have generally reported concentrations lower than those found here. In erythrocytes, Simons (1991) used $^{65}Zn^{2+}$ flux to arrive at an estimate of 1.5–32 pM for $[Zn^{2+}]_i$, depending on the ionic composition of the extracellular solution; in human leukemic cells, a $[Zn^{2+}]_i$ of ~1 nM was determined by ^{19}F nuclear magnetic resonance (Adebodun and Post, 1995). Additionally, fura-2-monitored $[Zn^{2+}]_i$ increased from 0.4 to 2 nM in chromaffin cells on electrical stimulation (Atar et al., 1995). However, recently zinquin was used to estimate concentrations of ~20–50 μM for $[Zn^{2+}]_i$ in splenocytes and thymocytes at rest (Zalewski et al., 1993) and of 0.6 to 2.7 μM in hepatocytes removed from rats fed a high-zinc diet (Brand and Kleineke, 1996).

In summary, we make one comment about methods and one comment about cellular Zn^{2+} homeostasis. First, although mag-fura-5 appears to provide a reasonable tool for measuring $[Zn^{2+}]_i$ dynamically in living neurons, especially when extracellular Ca^{2+} and Mg^{2+} are absent, such measurements will need to be interpreted cautiously, and all measurements made with mag-fura-5 will need confirmation once truly Zn^{2+}-selective ratioable dyes are available. Second, the observations presented here add to available evidence suggesting that Zn^{2+} can enter central neurons by multiple routes, likely in large part overlapping with routes of Ca^{2+} entry. Although the significance of this Zn^{2+} entry is most clearly defined in terms of contributing to the pathophysiology of neuronal degeneration in certain disease states, these mechanisms may also facilitate Zn^{2+} entry during normal synaptic transmission, permitting "transsynaptic messenger" Zn^{2+} to modulate a variety of processes in the postsynaptic neurons, such as signal transduction, transport processes, and gene expression (O'Halloran, 1993; Vallee and Falchuk, 1993).

REFERENCES

Adebodun F, Post JF (1995) Role of intracellular free Ca(II) and Zn(II) in dexamethasone-induced apoptosis and dexamethasone resistance in human leukemic CEM cell lines. J Cell Physiol 163:80–86.

Almers W, McClesley EW, Palade PT (1984) A non-selective cation conductance in frog muscle membrane blocked by micromolar external calcium ions. J Physiol (Lond) 353:565–583.

Andrews JC, Nolan JP, Hammerstedt RH, Bavister BD (1995) Characterization of *N*-(6-methoxy-8-quinolyl)-p-toluenesulfonamide for the detection of zinc in living sperm cells. Cytometry 21:153–159.

Armstrong CM, Lopez-Barneo J (1987) External calcium ions are re-

quired for potassium channel gating in squid neurons. Science 236:712–714.
Arslan P, Di Virgilio F, Beltrame M, Tsien RY, Pozzan T (1985) Cytosolic Ca^{2+} homeostasis in Erlich and Yoshida carcinomas. J Biol Chem 260:2719–2727.
Assaf SY, Chung SH (1984) Release of endogenous Zn^{2+} from brain tissue during activity. Nature 308:734–736.
Atar D, Backx PH, Appel MM, Gao WD, Marban E (1995) Excitation-transcription coupling mediated by zinc influx through voltage-dependent calcium channels. J Biol Chem 270:2473–2477.
Berg JM, Shi Y (1996) The galvanization of biology: a growing appreciation for the roles of zinc. Science 271:1081–1085.
Blaustein MP, Goldman WF, Fontana G, Krueger BK, Santiago EM, Steele TD, Weiss DN, Yarowsky PJ (1991) Physiological roles of the sodium–calcium exchanger in nerve and muscle. Ann NY Acad Sci 639:254–274.
Blaustein MP, Fontana G, Rogowski RS (1996) The Na(+)–Ca2+ exchanger in rat brain synaptosomes. Kinetics and regulation. Ann NY Acad Sci 779:300–317.
Brand IA, Kleineke J (1996) Intracellular zinc movement and its effect on the carbohydrate metabolism of isolated rat hepatocytes. J Biol Chem 271:1941–1949.
Brocard JB, Rajdev S, Reynolds IJ (1993) Glutamate-induced increase in intracellular free Mg^{2+} in cultured cortical neurons. Neuron 11:751–757.
Budde T, Minta A, White JA, Kay AR (1997) Imaging free zinc in synaptic terminals in live hippocampal slices. Neuroscience 79:347–358.
Choi DW, Maulucci-Gedde MA, Kriegstein AR (1987) Glutamate neurotoxicity in cortical cell culture. J Neurosci 7:357–368.
Christine CW, Choi DW (1990) Effect of zinc on NMDA receptor-mediated channel currents in cortical neurons. J Neurosci 10:108–116.
Danscher G (1984) Do the Timm sulphide silver method and the selenium method demonstrate zinc in the brain? In: The neurobiology of zinc (Frederickson CJ, Howell GA, Kasarskis EJ, eds), pp 273–287. New York: Liss.
Denny MF, Atchison WD (1994) Methylmercury-induced elevations in intrasynaptosomal zinc concentrations: an ^{19}F-NMR study. J Neurochem 63:383–386.
Diebler H, Eigen M, Ilgenfritz G, Maass G, Winkler R (1969) Kinetics and mechanism of reactions of main group metal ions with biological carriers. Pure Appl Chem 20:93–115.
Ebadi M, Iversen PL, Hao R, Cerutis DR, Rojas P, Happe HK, Murrin LC, Pfeiffer RF (1995) Expression and regulation of brain metallothionein. Neurochem Int 27:1–22.
Erickson JC, Hollopeter G, Thomas SA, Froelick GJ, Palmiter RD (1997) Disruption of the metallothionein-III gene in mice: analysis of brain zinc, behavior, and neuron vulnerability to metals, aging, and seizures. J Neurosci 17:1271–1281.
Frame MD, Milanick MA (1991) Mn and Cd transport by the Na–Ca exchanger of ferret red blood cells. Am J Physiol 261:C467–C475.
Frederickson CJ (1989) Neurobiology of zinc and zinc-containing neurons. Int Rev Neurobiol 31:145–238.
Frederickson CJ, Moncrieff DW (1994) Zinc-containing neurons. Biol Signals 3:127–139.
Frederickson CJ, Kasarskis EJ, Ringo D, Frederickson RE (1987) A quinoline fluorescence method for visualization and assaying the histochemically reactive zinc (bouton zinc) in the brain. J Neurosci Methods 20:91–103.
Frederickson CJ, Hernandez MD, McGinty JF (1989) Translocation of zinc may contribute to seizure-induced death of neurons. Brain Res 480:317–321.
Freund WD, Reddig S (1994) AMPA/Zn^{2+}-induced neurotoxicity in rat primary cortical cultures: involvement of L-type calcium channels. Brain Res 654:257–264.
Fukuda J, Kawa K (1977) Permeation of manganese, cadmium, zinc, beryllium through calcium channels of an insect muscle membrane. Science 196:309–311.
Grynkiewicz G, Poenie M, Tsien RY (1985) A new generation of Ca^{2+} indicators with greatly improved fluorescence properties. J Biol Chem 260:3440–3450.
Hansen AJ (1985) Effect of anoxia on ion distribution in the brain. Physiol Rev 65:101–148.
Harrison NL, Gibbons SJ (1994) Zn^{2+}: an endogenous modulator of ligand-and voltage-gated ion channels. Neuropharmacology 33:935–952.
Haugland RP (1996) Handbook of fluorescent probes and research chemicals, Ed 6, pp 531–540. Eugene, OR: Molecular Probes.
Hechtenberg S, Beyersmann D (1993) Differential control of free calcium and free zinc levels in isolated bovine liver nuclei. Biochem J 289:757–760.
Hollmann M, Hartley M, Heinemann S (1991) Ca^{2+} permeability of KA-AMPA-gated glutamate receptor channels depends on subunit composition. Science 252:851–853.
Howell GA, Welch MG, Frederickson CJ (1984) Stimulation-induced uptake and release of zinc in hippocampal slices. Nature 308:736–738.
Illner H, McGuigan JAS, Luthi D (1992) Evaluation of mag-fura-5, the new fluorescent indicator for free magnesium measurements. Pflügers Arch 422:179–184.
Jonas P, Racca C, Sakmann B, Seeburg PH, Monyer H (1994) Differences in Ca^{2+} permeability of AMPA-type glutamate receptor channels in neocortical neurons caused by differential GluR-B subunit expression. Neuron 12:1281–1289.
Koh JY, Choi DW (1994) Zinc toxicity on cultured cortical neurons involvement of *N*-methyl-D-aspartate. Neuroscience 60:1049–1057.
Koh JY, Suh SW, Gwag BJ, He YY, Hsu CY, Choi DW (1996) The role of zinc in selective neuronal death after transient global cerebral ischemia. Science 272:1013–1016.
Manev H, Kharlamov E, Uz T, Mason RP, Cagnoli CM (1997) Characterization of zinc-induced neuronal death in primary cultures of rat cerebellar granule cells. Exp Neurol 146:171–178.
Maret W (1995) Metallothionein/disulfide interactions, oxidative stress, and the mobilization of cellular zinc. Neurochem Int 27:111–117.
Masters BA, Quaife CJ, Erickson JC, Kelly EJ, Froelick GJ, Zambrowicz BP, Brinster RL, Palmiter RD (1994) Metallothionein III is expressed in neurons that sequester zinc in synaptic vesicles. J Neurosci 14:5844–5857.
O'Halloran TV (1993) Transition metals in control of gene expression. Science 261:715–725.
Palmiter RD, Cole TB, Quaife CJ, Findley SD (1996) ZnT-3, a putative transporter of zinc into synaptic vesicles. Proc Natl Acad Sci USA 93:14934–14939.
Pellegrini-Giampietro DE, Zukin RS, Bennett MV, Cho S, Pulsinelli WA (1992) Switch in glutamate receptor subunit gene expression in CA1 subfield of hippocampus following global ischemia in rats. Proc Natl Acad Sci USA 89:10499–10503.
Perez-Clausell J, Danscher G (1985) Intravesicular localization of zinc in rat telencephalic boutons: a histochemical study. Brain Res 337:91–98.
Peters S, Koh J, Choi DW (1987) Zinc selectively blocks the action of *N*-methyl-D-aspartate on cortical neurons. Science 236:589–593.
Petrozzino JJ, Pozzo Miller LD, Connor JA (1995) Micromolar Ca^{2+} transients in dendritic spines of hippocampal pyramidal neurons in brain slice. Neuron 14:1223–1231.
Pruss RM, Akeson RL, Racke MM, Wilburn JL (1991) Agonist-activated cobalt uptake identifies divalent cation-permeable kainate receptors on neurons and glial cells. Neuron 7:509–518.
Rose K, Goldberg MP, Choi DW (1993) Cytotoxicity in murine neocortical cell culture. In: Methods in toxicology (Tyson, CA, Frazier JM, eds), pp 46–60. San Diego: Academic.
Sheardown MJ, Suzdak PD, Nordholm L (1993) AMPA, but not NMDA, receptor antagonism is neuroprotective in gerbil global ischaemia, even when delayed 24 hr. Eur J Pharmacol 236:347–353.
Simons TJB (1991) Intracellular free zinc and zinc buffering in human red blood cells. J Membr Biol 123:63–71.
Simons TJB (1993) Measurement of free Zn^{2+} ion concentration with the fluorescent probe mag-fura-2 (furaptra). J Biochem Biophys Methods 27:25–37.
Sloviter RS (1985) A selective loss of hippocampal mossy fiber Timm stain accompanies granule cell seizure activity induced by perforant path stimulation. Brain Res 330:150–153.
Smart TG, Xie X, Krishek BJ (1994) Modulation of inhibitory and excitatory amino acid receptor ion channels by zinc. Prog Neurobiol 42:393–441.
Tibbits GF, Philipson KD (1985) Na^{+}-dependent alkaline earth metal uptake in cardiac sarcolemmal vesicles. Biochim Biophys Acta 817:327–332.
Tonder N, Johansen FF, Frederickson CJ, Zimmer J, Diemer NH (1990) Possible role of zinc in the selective degeneration of dentate hilar neurons after cerebral ischemia in the adult rat. Neurosci Lett 109:247–252.

Turetsky DM, Canzoniero LMT, Sensi SL, Weiss JH, Goldberg MP, Choi DW (1994) Cortical neurons exhibiting kainate-activated Co^{2+} uptake are selectively vulnerable to AMPA/kainate receptor-mediated toxicity. Neurobiol Dis 1:101–110.

Vallee BL, Falchuk KH (1993) The biochemical basis of zinc physiology. Physiol Rev 73:79–118.

Vega MT, Villalobos C, Garrido B, Gandia L, Bulbena O, Garcia-Sancho J, Garcia AG, Artalejo AR (1994) Permeation by zinc of bovine chromaffin cell calcium channels: relevance to secretion. Pflügers Arch 429:231–239.

Verdoorn TA, Burnashev N, Monyer H, Seeburg PH, Sakmann B (1991) Structural determinants of ion flow through recombinant glutamate receptor channels. Science 252:1715–1718.

Wang YX, Quastel DM (1990) Multiple actions of zinc on transmitter release at mouse end-plates. Pflügers Arch 415:582–587.

Weiss JH, Hartley DM, Koh JY, Choi DW (1993) AMPA receptor activation potentiates zinc neurotoxicity. Neuron 10:43–49.

Westbrook GL, Mayer ML (1987) Micromolar concentrations of Zn^{2+} antagonize NMDA and GABA responses of hippocampal neurons. Nature 328:640–643.

Yin HZ, Weiss JH (1995) Zn^{2+} permeates Ca^{2+} permeable AMPA/kainate channels and triggers selective neural injury. NeuroReport 6:2553–2556.

Yin HZ, Turetsky DM, Choi DW, Weiss JH (1994) Cortical neurons with Ca^{2+} permeable AMPA/kainate channels display distinct receptor immunoreactivity and are GABAergic. Neurobiol Dis 1:43–49.

Yokoyama M, Koh JY, Choi DW (1986) Brief exposure to zinc is toxic to cortical neurons. Neurosci Lett 71:351–355.

Yu SP, Choi DW (1997) Na^{+}-Ca^{2+} exchange currents in cortical neurons: concomitant forward and reverse operation and effect of glutamate. Eur J Neurosci 9:1273–1281.

Zalewski PD, Forbes IJ, Betts WH (1993) Correlation of apoptosis with change in intracellular labile Zn(II) using Zinquin [(2-methyl-8-*p*-toluesulphonamido-6-quinolyloxy)acetic acid], a new specific fluorescent probe for Zn(II). Biochem J 296:403–408.

Zalewski PD, Millard SH, Forbes IJ, Kapaniris O, Slavotinek A, Betts WH, Ward AD, Lincoln SF, Mahadevan I (1994) Video image analysis of labile zinc in viable pancreatic islet cells using a specific fluorescent probe for zinc. J Histochem Cytochem 42:877–884.